

Finite element simulation of composite steel-concrete castellated and cellular beams: effect of the web openings

Matheus E. Benincá¹, Inácio B. Morsch¹

¹*Programa de Pós-Graduação em Engenharia Civil, Universidade Federal do Rio Grande do Sul
Av. Osvaldo Aranha, 99, 90035-190, Porto Alegre/RS, Brasil
matheuseb@hotmail.com, morsch@ufrgs.br*

Abstract. Composite castellated or cellular beams consist of a concrete slab linked with castellated or cellular steel profiles through shear studs. Particularly, for simply supported beams, it results in an optimized structural solution. However, designing a composite alveolar beam is not a simple task, since Brazilian and international standards do not specify criteria for its analysis and design. Therefore, advances in numerical simulations are important for a better understanding of their complex structural behavior, which involves different failure modes. This work continues the research presented in the latest edition of CILAMCE, in which a finite element model was developed and validated, using ANSYS software. This model was used in this paper to study the effects of the web openings on the structural behavior of composite beams. For this purpose, firstly two composite cellular beams experimentally tested in previous works were numerically simulated, considering the cases with and without web openings. Secondly, it was proposed an example of a beam with a larger span (11 m) subjected to a uniformly distributed load, and a numerical study was carried out considering both the original steel profile, without holes, and the expanded profiles, with different opening patterns. It was concluded that the web-post buckling may limit the structural gains on load capacity, so it is important to adopt opening patterns that enhance the resistance of the beam to this mode of failure. On the other hand, when the failure mode is the formation of a flexural mechanism, it was verified that the load capacity gain is influenced by the expansion ratio and the tee-section height.

Keywords: Composite cellular beams, composite castellated beams, web-post buckling, finite element method.

1 Introduction

The use of composite alveolar beams allows to simultaneously benefit from the structural advantages of steel-concrete composite beams and alveolar steel profiles, enabling the design of larger spans and the achievement of more economical and sustainable solutions.

According to Badke-Neto et al. [1], depending on the shape of the openings, the alveolar steel beams can be named as castellated beams (with hexagonal openings) or cellular beams (with circular openings). Their manufacturing process consist in cutting the original steel profile longitudinally in a certain pattern, resulting in two parts that can be repositioned and then welded together in a new configuration, in which the flanges are farther apart. Thus, with practically the same weight, the expanded profiles are produced with a greater moment of inertia and, consequently, greater flexural strength, resulting in a better performance under serviceability limit states.

The cut pattern adopted determines the opening pattern and its respective geometric parameters. In the case of castellated beams, the most adopted patterns are called Litzka, Anglo-Saxon and Peiner. The geometric parameters of each pattern strongly influence the failure mode of the beam, which, according to Kerdal and Nethercot [2], can be one of the modes following listed: (i) Formation of a Vierendeel mechanism; (ii) Buckling of web-post due to shear; (iii) Rupture of a welded joint in a web-post; (iv) Lateral-torsional buckling of an entire span; (v) Formation of a flexural mechanism (plastic hinge); and (vi) Buckling of web-post due to compression.

Regarding the composite alveolar beams, the presence of a concrete slab can modify the failure modes and even create new modes, involving concrete crushing or excessive concrete cracking. In this context, Redwood [3] outlined that once the composite action increases the resistances to flexural and Vierendeel mechanisms, there is

an increased likelihood of web-post buckling in composite castellated sections. Thus, the resistance of these beams to failure modes involving local instabilities is a fundamental issue to be investigated. It is worth mentioning that the Brazilian standard NBR 8800:2008 [4] and the most well-known international standards, such as EN 1994-1-1:2004 [5] and ANSI/AISC 360-16 [6], do not directly specify criteria for the analysis and design of composite castellated or cellular beams considering their specific modes of failure.

Therefore, advances in numerical simulation are essential for a better understanding of the structural behavior of composite alveolar beams and can be helpful for the validation and improvement of future standardizations. In a previous work (Benincá and Morsch [7]), a finite element model was developed and validated, using ANSYS software, version 19.2. This model will be used in this paper to investigate the effect of the web openings on the structural behavior of composite beams.

Thus, it is proposed to compare the structural behavior of composite alveolar beams to the behavior of similar composite beams with the respective full web profiles. This study will be carried out for: (i) composite cellular beam A1 tested by Nadjai et al. [8], with a span of 4,50 m and subjected to a concentrated load; (ii) composite cellular beam tested by Müller et al. [9], with a span of 6,84 m and subjected to a set of concentrated loads along the span; and (iii) numerical example of a beam with a span of 11 m and subjected to a uniformly distributed load, considering different opening patterns in the web.

2 Numerical Model

The three-dimensional numerical model was developed in ANSYS software, version 19.2, and was described in greater detail in a previous work (Benincá and Morsch [7]), in which it was validated. Table 1 summarizes the element types adopted for each component of the composite beams, as well as the material models used. Figure 1 shows the boundary conditions adopted, for both cases with and without symmetry. A concentrated load was preferably applied by imposing y-displacements on the respective nodes, at the top face of the slab, once, as outlined by Queiroz et al. [10], the displacement control may overcome convergence problems. However, as explained by these authors, in cases of distributed loads, or of a set of multiple concentrated loads, it is necessary to apply forces, since in these cases it is difficult to establish a relation between loads and the associated displacements, especially during the plastic range of behavior.

Table 1. Element types and material models adopted in ANSYS model, as in Benincá and Morsch [7].

Component	Element Type	Material Model
Steel Profile	4-node SHELL181	von Mises, nonlinear hardening [11]
Steel-Deck Sheet	8-node SHELL281	von Mises, perfect elastoplastic
Concrete Slab	20-node SOLID186	Drucker-Prager (compression) and Rankine (tension)
Reinforcement bars	Embedded REINF264	von Mises, perfect elastoplastic
Connectors	Spring COMBIN39	Nonlinear relationship for shear force versus slip

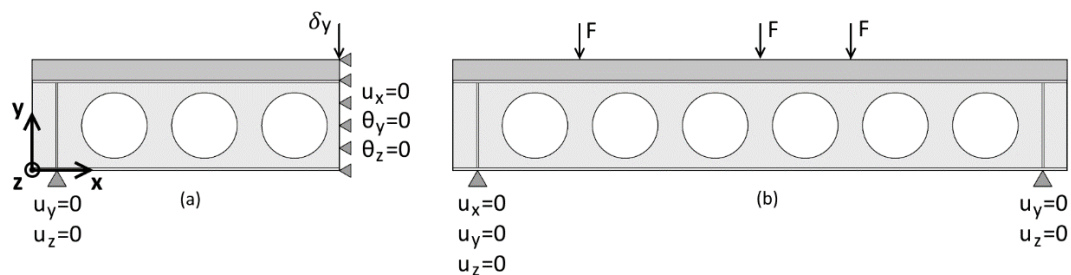


Figure 1. Boundary conditions: (a) with symmetry; (b) without symmetry.

To simulate the failure modes involving local instabilities, the analysis was performed in four stages:

(1) *Solution of a linear static analysis*, in which a unit load was distributed among the same nodes of the load that is applied in the final analysis.

(2) *Solution of an Eigen-Buckling analysis*, which consists in a linear eigenvalue problem (Bathe [12]) to determine the buckling modes and the load factors associated with the linear static analysis performed in stage 1.

(3) *Insertion of geometric imperfections to the steel profile*, by updating the model geometry, based on the buckling modes (eigenvectors) calculated at stage 2. The weighted combination of two buckling modes was applied, with an amplitude of $d_g/600$ each (Bake [13]), where d_g is the height of the expanded profile.

(4) *Solution of the nonlinear analysis*. When the load was applied by imposing equivalent displacements, the full Newton-Raphson method with displacement control was used to solve the nonlinear problem. Otherwise, when forces were applied, the Arc-Length method was adopted, aiming to capture the post-buckling behavior, since the Newton-Raphson method with force control does not support sudden changes in the structure stiffness that lead to negative force increments.

3 Examples analyzed

The geometry of the composite cellular beam A1 [8] is shown in figure 2. This beam has a free span of 450 cm, is symmetrical and has been subjected to two symmetrical concentrated loads. The original steel profile is UB 406x140x39, and the expansion ratio (ratio between the height of the expanded profile and the original profile) is 1,445. The yield and ultimate strengths of steel are 31.20 kN/cm² and 43.85 kN/cm², respectively. The concrete's mean uniaxial compressive strength (f_{cm}) is equal to 3.50 kN/cm². More details about this beam can be found in Nadjai et al. [8] and in Benincá and Morsch [7].

The geometry of the composite cellular beam 1 [9] is also shown in figure 2. This beam has a free span of 684 cm, is not symmetrical (due to the non-concreted right corner) and was subjected to four concentrated loads along the span. Beam 1 was tested twice: in the first test (named 1A) the beam has failed by web-post buckling due to shear, close to the second support. When the buckling started, the beam was unloaded, and then the web was stiffened in this location with a rigid bar. Next, a new test was carried out (named 1B). The original steel profile is IPE400, and the expansion ratio is 1.388. The yield and ultimate steel strengths are 48.90 kN/cm² and 58.68 kN/cm², respectively. The concrete's mean uniaxial compressive strength (f_{cm}) is equal to 4.20 kN/cm². More details about this beam can be found in Müller et al. [9].

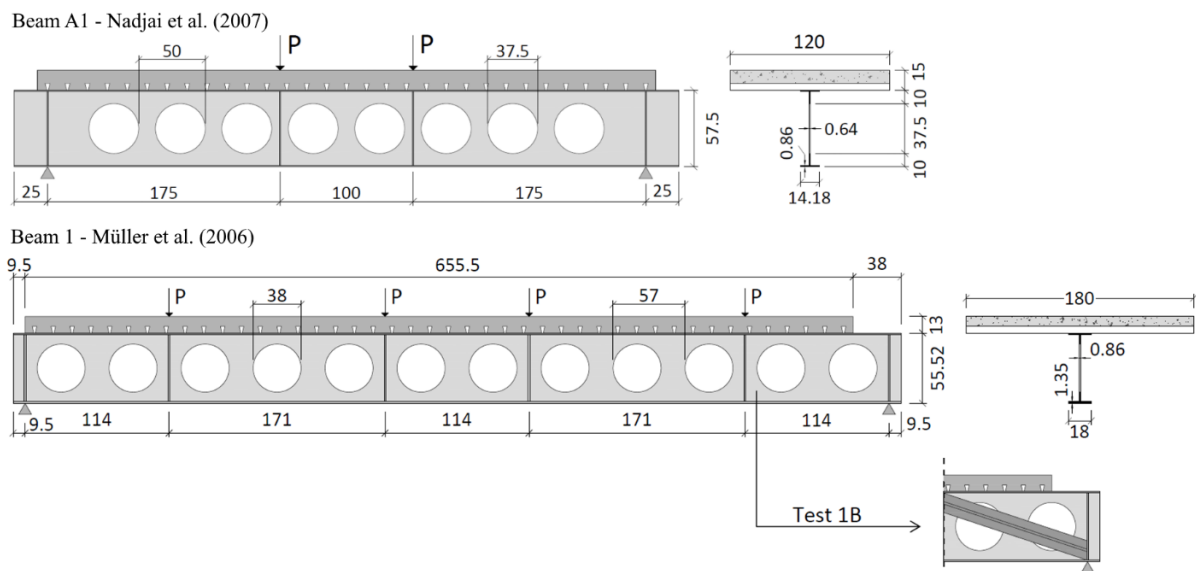


Figure 2. Geometries of beam A1 [8] and beam 1, in tests 1A and 1B [9]

For each one of these beams, three numerical analyses were performed: one simulating the experiment, with the expanded steel profile, another of a composite beam with the original steel profile, before expansion, and another for a composite beam considering a fictional expanded profile, without openings.

However, it is known that the application of composite alveolar beams generally occurs for larger spans than those of the previous examples. Once experimental tests with larger spans were not found in literature, it was

necessary to create a new example to be analyzed. Therefore, it was proposed the case of a beam with 11m span, subjected to a uniformly distributed load. The other geometric characteristics and material properties were admitted, for simplification purposes, as being the same as those of beam 1 by Müller et al. [9]. IPE400 profile was used as the original steel profile, and expansions with different opening patterns were analyzed. Figure 3 shows the nomenclature adopted for the geometric parameters, and Table 2 presents the names adopted for the beams and their respective geometric parameters. Composite beams with full web profiles were named FW1 and FW2. The proposed composite castellated beams cover the most usual patterns, called Litzka (CA1), Anglo-Saxon (CA2) and Peiner (CA3). The proposed composite cellular beams have different ratios s/D_0 , assuming the values of 1.1 (CE1), 1.2 (CE2), 1.3 (CE3) and 1.4 (CE4), all of them with a diameter of 44 cm and expansion ratio $k=1.5$. The beam CE5 has a smaller diameter (38 cm), $s/D_0=1.5$, and expansion ratio $k=1.388$, as in the pattern used by Müller et al. [9] in beam 1. All these beams were numerically analyzed considering the symmetry condition.

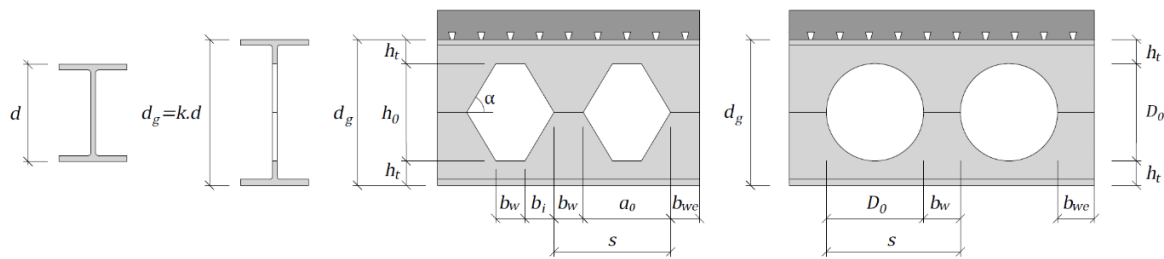


Figure 3. Nomenclature adopted for the geometric parameters of castellated and cellular beams.

Table 2. Beams analyzed for the example of 11 m span.

Beam	Steel Profile	k	h_0 [cm]	a_0 [cm]	D_0 [cm]	s [cm]	b_w [cm]	b_t [cm]	h_t [cm]
FW1	Original IPE400, $d=40$ cm	1	-	-	-	-	-	-	-
FW2	Expanded, without holes	1.5	-	-	-	-	-	-	-
CA1	Castellated Litzka	1.5	40	46.19	-	69.28	23.09	11.55	10
CA2	Castellated Anglo-Saxon	1.5	40	33.15	-	43.20	10.05	11.55	10
CA3	Castellated Peiner	1.5	40	40.00	-	60.00	20.00	10.00	10
CE1	Cellular, $s/D_0=1.1$	1.5	-	-	44	48.40	4.40	-	8
CE2	Cellular, $s/D_0=1.2$	1.5	-	-	44	52.80	8.80	-	8
CE3	Cellular, $s/D_0=1.3$	1.5	-	-	44	57.20	13.20	-	8
CE4	Cellular, $s/D_0=1.4$	1.5	-	-	44	61.60	17.60	-	8
CE5	Cellular, $s/D_0=1.5$	1.388	-	-	38	57.00	19.00	-	8.8

The mapped mesh of the steel profile was generated with the maximum element size criterion, with this value varying between 3 and 4 cm in the examples with alveolar profiles, and around 6 cm in the examples with full web profiles. Beam A1 [8] was modeled with the symmetry condition, and the concentrated load was applied by imposing displacements in y direction, making it possible to use the Newton-Raphson method with displacement control in the nonlinear solution and, even so, to capture the post-buckling behavior. On the other hand, in the beams of Müller et al. [9] and in the beams of the proposed example with 11 m span, since they are subjected, respectively, to a set of loads and to a distributed load, it was necessary to apply the loads as forces, and in this case it was decided to use the Arc-Length method with force control to capture post-buckling behavior.

4 Results and discussion

A comparison between the numerical and experimental results of the composite cellular beam A1 [8] and its respective composite beams with full web profiles (UB 406x140x39 original profile and an expanded profile without holes) is shown in Figure 4. It is observed that in this example the stiffness gain obtained with the expansion of the original profile is not significant, possibly due to its small free span (4.5 m, as shown in Figure

2), so that shear forces are considerable in comparison to the bending moments. In addition, it can be noted that there is a decrease in the ultimate load capacity, since the composite cellular beam failed by web-post buckling due to shear, which occurred at the load of 351.92 kN (numerical) and 370.12 (experimental). Therefore, from a structural point of view, in this case there are no great advantages in expanding the steel profile. However, in a real project this expansion could be considered for other reasons, such as the passage of ducts and pipes or the achievement of a lighter design.

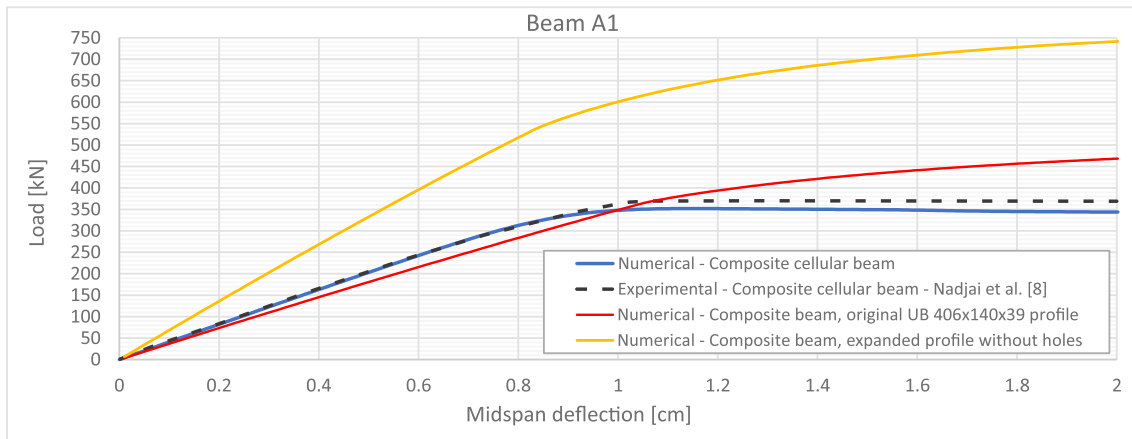


Figure 4. Load-deflection curves: composite beams and composite cellular beam A1.

Figure 5 shows the numerical and experimental results of the composite cellular beam 1 [9] compared to the two composite beams with full web profiles considered (IPE400 original profile and an expanded profile without holes). Differently from the previous example, in this case it is already possible to notice a greater gain in initial stiffness, which occurs because the span is larger (6.84 m, as shown in Figure 2), and the four concentrated loads are distributed along the span, simulating a uniformly distributed load.

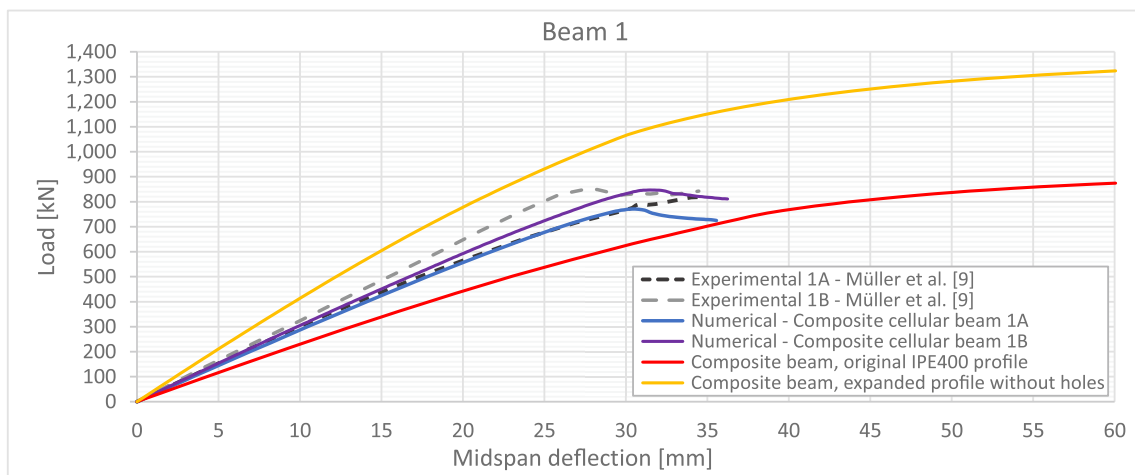


Figure 5. Load-deflection curves: composite beams and composite cellular beams 1A and 1B.

Table 3. Load applied when midspan deflection is equal to $L/250 = 27.4$ mm.

Beam	Load when $u_y=27.4$ mm [kN]	Relative difference
Composite beam with original IPE400 profile	580.50	-
Composite cellular beam 1A	728.07	+ 25.42%
Composite cellular beam 1B	733.87	+ 26.42%
Composite beam, expanded profile without holes	998.09	+ 71.94%

Table 3 presents the loads corresponding to a midspan deflection of 27.4 mm (equal to $L/250$), and it is observed that the profile expansion generates a gain of load equal to 25.42% in test 1A and 26.42% in test 1B. However, it can be once more verified that, in terms of ultimate behavior, the web-post buckling limited the possible gains in ultimate load capacity.

Figure 6 presents the results obtained for the load-deflection curves of all cases considered in the proposed example with 11m free span. As it can be observed, all beams with expanded profiles, except for beam CE1, had significant gains in initial stiffness. Table 4 presents the applied linear load values for a midspan deflection of 44 mm (equal to $L/250$), showing the mentioned gain. Due to the smaller expansion ratio $k = 1.388$ of beam CE5, it presented lower gains than CE4, CA1, CA2 and CA3 beams. At the same time, beam CE4, with an expansion ratio $k=1.5$, had a greater gain than beam CE5, but slightly smaller than in the castellated beams. It has occurred because, despite having profiles with equal height ($d_g = 1.5 \times 40 = 60$ cm), the heights of the tee-sections are different due to the manufacturing process in double cut (cellular beams) or single cut (castellated beams). On the other hand, the composite castellated beams CA1, CA2 and CA3 presented similar results to each other, once their expanded profiles have not only the same height d_g , but also the same tee-section height h_t .

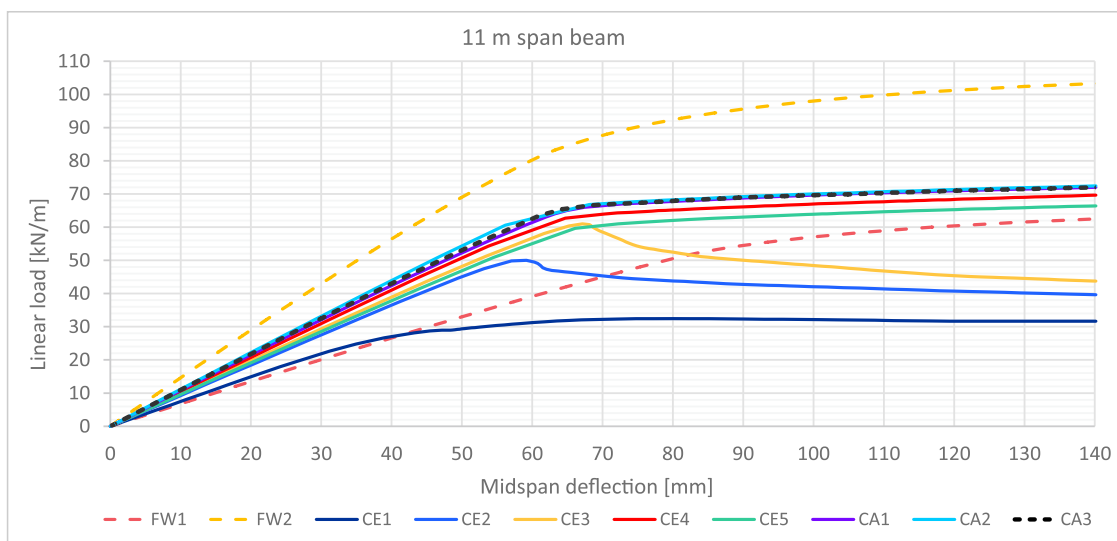


Figure 6. Load-deflection curves for the beam with 11m span.

Table 4. Linear load applied when the midspan deflection is equal to $L/250 = 44$ mm.

$u_y=44\text{mm}$	FW1	FW2	CA1	CA2	CA3	CE1	CE2	CE3	CE4	CE5
q [kN/m]	29.17	61.60	46.38	48.12	47.08	28.35	39.96	42.68	44.99	41.52
Rel. diff.	-	111.18%	59.00%	64.96%	61.40%	-2.81%	36.99%	46.31%	54.23%	42.34%

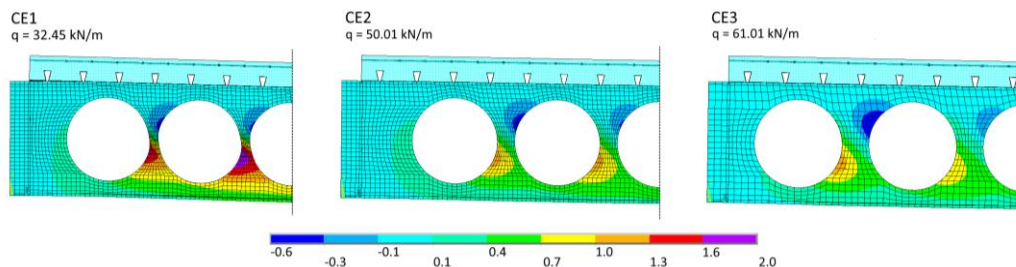


Figure 7. Web-post buckling in beams CE1, CE2 and CE3 (transversal displacements, in cm).

With respect to the ultimate behavior, beams CE1, CE2 and CE3 failed early by web-post buckling due to shear, thus in these three cases the gain in load capacity was limited. This failure mode occurred in these beams due to the slenderness of their web-posts, which increases with the decrease of the s/D_0 ratio, resulting in a greater

susceptibility for the occurrence of buckling. Figure 7 shows the out-of-plane displacements for these three beams, at their respective ultimate loads (32.45 kN/m, 50.01 kN/m and 61.01 kN/m).

Regarding the other composite alveolar beams results (CE4, CE5, CA1, CA2, CA3), it can be observed that there was a gain not only in the initial stiffness but also in the ultimate load, when compared to the composite beam with the original steel profile (FW1). It has occurred because these beams failed by the formation of a flexural mechanism, for which increasing the height of the profile also increases its load capacity.

Therefore, from this example it can be noted that the expansion of the profile may lead to a significant gain in initial stiffness, resulting in a better performance under serviceability limit states. More than that, it may also increase the ultimate load if web-post buckling is not the predominant failure mode. Thus, when designing a composite alveolar beam, it is important to adopt an opening pattern that presents greater resistance to this mode of failure, for example with larger web-posts and greater s/D_0 ratios.

5 Conclusions

In this paper, a study about the effect of the web openings on the behavior of composite beams was carried out, using a finite element model developed and validated in a previous work [7]. From the obtained results, it can be concluded that:

- The structural gains due to steel profile expansion become more significant in larger spans.
- The gains in load capacity may be limited when the failure mode is web-post buckling. Thus, when designing composite alveolar beams, it is important to ensure a great resistance to this failure mode.
- When the failure mode is the formation of a flexural mechanism, the load capacity gain is influenced by the expansion ratio and the tee-section height.

Acknowledgements. The authors are grateful to CAPES and CNPq for the financial support for this research, and to CEMACOM/UFRGS for providing the infrastructure for the development of this work.

Authorship statement. The authors hereby confirm that they are the sole liable persons responsible for the authorship of this work, and that all material that has been herein included as part of the present paper is either the property (and authorship) of the authors, or has the permission of the owners to be included here.

References

- [1] A. Badke-Neto, A. F. G. Calenzani and W. G. Ferreira, “Study of methods for the design of cellular composite steel and concrete beams”. *Rev. IBRACON Estrut. Mater.*, vol. 8, n. 6, pp. 827–859, 2015.
- [2] D. Kerdal and D. A. Nethercot, “Failure modes for castellated beams”. *J. Constr. Steel Res.*, vol. 4, pp. 295–315, 1984.
- [3] R. G. Redwood, “Behaviour of composite castellated beams”. *Progr. Struct. Eng. Mater.*, vol. 2 n. 2, pp. 164–168, 2000.
- [4] ABNT. *NBR 8800: Projeto de estruturas de aço e de estruturas mistas de aço e concreto de edifícios*. Rio de Janeiro, 2008.
- [5] CEN. *EN 1994-1-1: Eurocode 4: Design of composite steel and concrete structures – Part 1-1*. Brussels, 2004.
- [6] AISC. *ANSI/AISC 360-16: Specification for Structural Steel Buildings*. Chicago, 2016.
- [7] M. E. Benincá and I. B. Morsch, “Development of a finite element model of steel-concrete composite alveolar beams”. In: *XL Ibero-Latin-American Congress on Computational Methods in Engineering*, Natal, 2019.
- [8] A. Nadjai, O. Vassart, F. Ali, D. Talamona, A. Allam, and M. Hawes, “Performance of cellular composite floor beams at elevated temperatures”. *Fire Saf. J.*, vol. 42, pp. 489–497, 2007.
- [9] C. Müller, O. Hechler, A. Bureau, D. Bitar, D. Joyeux, L. G. Cajot, T. Demarco, R. M. Lawson, S. Hicks, P. Devine, O. Lagerqvist, E. Hedman-Pétursson, E. Unosson, and M. Feldmann (2006). *Large web opening for service integration in composite floors: final report*. Office for Official Publications of the European Communities, 2006.
- [10] F. D. Queiroz, P. C. G. S. Vellasco and D. A. Nethercot, “Finite element modelling of composite beams with full and partial shear connection”. *J. Constr. Steel Res.*, vol. 63, pp. 505–521, 2007.
- [11] N. Gattesco, “Analytical modeling of nonlinear behavior of composite beams with deformable connection”. *J. Constr. Steel Res.* 52:195–218, 1999.
- [12] K. J. Bathe. *Finite element procedures*. KJ Bathe, 2nd ed., 2014.
- [13] S. Bake. *Behaviour of cellular beams and cellular composite floors at ambient and elevated temperatures*. PhD thesis, University of Manchester, 2010.